Jestr

Journal of Engineering Science and Technology Review 17 (3) (2024) 1-7

Research Article

JOURNAL OF
Engineering Science and Technology Review

www.jestr.org

Modeling the Link Between Electric Fields and Three Films of Porous Channel Flow

Azizah Alrashidi and Sameh A. Alkharashi*

Department of Laboratory Technology, College of Technological Studies, PAAET, Kuwait

Received 3 April 2024; Accepted 7 June 2024

Abstract

In the presence of stream periodicity, the electrohydrodynamic instability of three bounded liquid films with two interfaces is examined. It is considered that liquids have distinct physical characteristics and are immiscible. Under the influence of an electric horizontal field, these fluids travel through porous material. Applying the linear theory to the equations of motion and the associated boundary conditions led to two coupled Mathieu type equations with complex periodic coefficients. Approximate solutions were achieved by employing the multiple time scales technique, where the stability performance in resonance cases or not was discussed. An essential feature of this method is that transition curves are obtained analytically. It was discovered that all of the points inside these curves are unstable, whereas the regions outside of them promote the system's stability. A detailed analysis is conducted to determine how the different physical variables of the problem affect the interface stability. In the case of uniform speed, it is observed that the electric field stimulates the stability of the wave motion, while the porosity of the upper layer plays a dual role. In the presence of periodic speeds, it was observed that the speed of the top film works to destabilize the waves, while the dielectric constant gives brightness to the stability of the waves. It is also mentioned that the electric field has an important and effective role in stabilizing the fluid layers.

Keywords: Electrohydrodynamics; Liquid layers; Porous media; Mathieu equations.

1. Introduction

Stability is a significant and useful issue in many industrial applications, such as some areas of petroleum, chemical, and mechanical engineering. The manufacture of steel and alloys, as well as coating operations, demonstrate the significance of the stabilizing process. Additionally, it is preferable for some alloys to remain bubble-free throughout manufacturing because this adds to their worth and quality; otherwise, it could seriously impair the final product's quality.

The presentation of various pertinent studies that provide a useful summary of hydrodynamic stability is provided below. Ozen et al. [1] performed two layers of different fluids containing an interface. The imposed fluids are viscous and move under the influence of a perpendicular electric field. Investigations into the effects of various physical quantities on the stability of the interface revealed that, while the electric field helps to stabilize the movement, it sometimes works on the opposite. The method described in [2] involves examining the effect of an electric field that is perpendicular to a channel that contains various viscous fluids and confines an interface. The stability of the problem was achieved based on the long-wave theory. It was indicated that the effect of the electric field depends on whether it is perfect or leaky dielectrics.

In article [3], the linear stability investigation of pressure-driven flow under viscous heating effect via a channel is carried out. A modified coupled Orr–Sommerfeld equation was obtained with a linearized energy equation. It was mentioned that viscous heating has a destabilizing impact. DiCarlo [4] has theoretically investigated the stability of the standard multiphase flow equations. However, he has demonstrated experimentally that the instability is associated with saturation or pressure overshoot occurrences in 1-D infiltrations. The effect of fluid characteristics and flow was examined in the research of the movement of multi-layered fluids under the influence of fields in porous media, which can be found in the work of [5-7].

The linear stability theorem is applied in the work of [8] to describe the motion of two layers of Herschel–Bulkley and immiscible Newtonian fluids. It has been suggested that the applied electric field can either play a stable or unstable function for the channel motion, depending on the electrical properties of the fluids. The linear stability analysis for an electrically charged fluid sheet sandwiched between two symmetric dielectric moveable ambient gases has been examined in [9]. The findings show that, for the sinuous type, the tangential field stabilizes the system over the complete range of the gas speed ratio, and that, for the varicose mode, the electric field marginally improves the stability performance. Finally, good accounts of the subject under study can be discerned in the literature [10-20].

Drawing on the previously given information, we examine in this study, the linear stability of a sheet made up of three distinct fluid films enclosing two interfaces. Fluids flow through porous media while being subjected to a periodic velocity in the direction of the fluid layers and a horizontal electric field. The results obtained here may be of interest in some scientific issues related to industries and modern technology such as plastics manufacture lubricants, as well as many spray coating processes. It is worth noting that the concept of stability is of great importance in the process of painting surfaces and walls, as the paints remain adhered to the walls and does not peel off them, even in different weather conditions such as temperature and humidity.

The current article is prepared as follows. In the subsequent section, the problem statement is evidently covered, and the important equations of motion and the linked

*E-mail address: sa.alkharashi@paaet.edu.kw
ISSN: 1791-2377
doi:10.25103/jestr.173.01

boundary requirements have been analyzed. The third section is devoted to the perturbed motion and solutions to the problem. In the fourth section, the characteristic equations and stability performance is covered. The notable results are presented in the last section.

2 Problem statement

In the current model, two bounded electrical fluids with different physical properties for each of the three fluids are sandwiched between an electrical layer of a fluid sheet. It is assumed that all fluids move in an infinite horizontal direction with a periodic velocity through porous media. Fig. 1 depicts a geometric visualization of the hypothesized model for the study, where gravity acts downward.

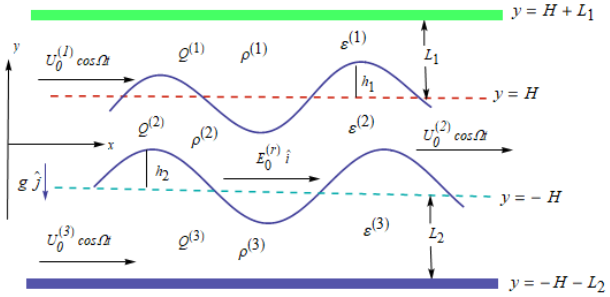

Fig. 1. Geometrical representation of the imposed system.

Initially, the separating surfaces between the fluids are undistributed, and we have a middle region $-H < y < H$, moreover, two bounded regions, the upper confined between $H < y < H + L_1$ and the other is the lower layer in the range $-H < y < -(H + L_2)$. The periodic form of the velocity through the fluid sheet is given as $U_0^{(r)}\cos\Omega t$ growing in the $x-$ axis direction, where $U_0^{(r)}$, Ω are constants. The superscript $r = 1, 2, 3$ distinguishes the three layers from top to bottom. If $h_l(x,t)$ indicates the height above the undisturbed plane and based on visualizing motion in two dimensions, the resulting distortion at the two interfaces can be expressed as follows:

$$y(x,t) = (-1)^{(l+1)}H + h_l(x,t),\ l = 1, 2. \tag{1}$$

The equations of motion and the suitable boundary conditions for the imposed system can be mentioned as follows. Fluids are assumed to obey Darcy's law, and therefore the governing equation results from the combination of this law and the momentum equation, so that [21-27]:

$$\rho^{(r)}D_t\boldsymbol{u}^{(r)} = -\nabla p^{(r)} + \eta^{(r)}{Q^{(r)}}^{-1}\boldsymbol{u}^{(r)} - \rho^{(r)}(g, 0), \tag{2}$$

the continuity equation of homogeneous liquid reads:

$$\nabla \cdot \boldsymbol{u}^{(r)} = 0. \tag{3}$$

Here, $D_t = \partial_t + \left(\boldsymbol{u}^{(r)} \cdot \nabla\right)$ states the material differential operator, and the subscripts t, x and y identify the partial derivatives. The parameter $\nabla \equiv (\partial x, \partial y)$ distinguishes the horizontal gradient operator. The quantity $\eta^{(r)}{Q^{(r)}}^{-1}$ is the resistance parameter, where $Q^{(r)}$ characterizes the permeability of the porous medium and $\eta^{(r)}$ denotes the fluid viscosity. The value $p^{(r)}$ indicates the fluid pressure and the symbol $\rho^{(r)}$ indicates the density of the lquids films.

Given that the assumed fluids are inviscid and therefore irrotational, then it is possible to talk about a streaming potential for the perturbed motion, and the total velocity is intended based on following relationship:

$$\boldsymbol{u}^{(r)} = \left(U_0^{(r)}\cos\Omega t - \partial_x\phi^{(r)}(x,y,t) \quad -\partial_y\phi^{(r)}(x,y,t)\right)\begin{pmatrix}\hat{\boldsymbol{\imath}}\\ \hat{\boldsymbol{\jmath}}\end{pmatrix}, \tag{4}$$

where, $\hat{\boldsymbol{\imath}}$ and $\hat{\boldsymbol{\jmath}}$ are unit vectors in $x-$ and $y-$ directions. In this case, $\phi^{(r)}$ will fulfill Laplace equation

$$\nabla^2\phi^{(r)}(x,y,t) = 0. \tag{5}$$

If there are no free currents, Maxwell's equations have the form

$$\nabla.(\varepsilon^{(r)}\boldsymbol{E}^{(r)}) = 0 \text{ and } \nabla \times \boldsymbol{E}^{(r)} = 0, \tag{6}$$

where, the parameter $\varepsilon^{(r)}$ indicates the dielectric constant and $\boldsymbol{E}^{(r)} = (E_x^{(r)}, E_y^{(r)})$ designates the electric field vector. From the previous two field equations, a scalar field potential $\psi^{(r)}$ can be formulated in the form:

$$\boldsymbol{E}^{(r)} = \left(E_0^{(r)} - \partial_x\psi^{(r)}(x,y,t) \quad -\partial_y\psi^{(r)}(x,y,t)\right)\begin{pmatrix}\hat{\boldsymbol{\imath}}\\ \hat{\boldsymbol{\jmath}}\end{pmatrix}, \tag{7}$$

Given that we have a constant permittivity, the zero curl holds, and consequently the electrostatic potential matches Laplace's equation so that:

$$\nabla^2\psi^{(r)} = 0. \tag{8}$$

Now we are dealing with the boundary conditions, which are information at the dividing surfaces and the upper and lower boundary [28-32]. At the upper and lower surfaces, we discuss the kinematic condition, which results from the fact that the separating surface always includes the same fluid particles.

$$D_t[y - (-1)^{(l+1)}H - h_l] = 0 \tag{9}$$

Alongside this condition, another important condition appears, which is the continuity of the perpendicular component to the speed at the separating surfaces, where:

$$\boldsymbol{n}_l \cdot \| \boldsymbol{u}^{(l,l+1)} \| = 0 \tag{10}$$

Here, $\boldsymbol{n}_l$ indicates the exterior normal unit vector to the dividing surfaces which is linearly typified by $\boldsymbol{n}_l = -\partial_x h_l\hat{\boldsymbol{\imath}} + \hat{\boldsymbol{\jmath}}$. The representation $\| \cdots \|$ indicates a jump in any measure through the separated surfaces.

Another condition that can be noted is the lack of speeds at the upper and lower plates due to the border being fixed and rigid. This is recorded at the upper and lower bounds, respectively:

$$\left.\begin{aligned} u^{(1)} &= 0 \ \text{ at } \ y = L_1,\\ u^{(2)} &= 0 \ \text{ at } \ y = -L_2. \end{aligned}\right\} \tag{11}$$

In light of Maxwell's conditions, the perpendicular and tangential components of the field are connected and can be formulated as:

$$[\varepsilon^{(l)}E_0^{(l)} - \varepsilon^{(l+1)}E_0^{(l+1)}]\partial_x h(x,t) = \varepsilon^{(l+1)}\partial_y\psi^{(l+1)} - \varepsilon^{(l)}\partial_y\psi^{(l)}, \tag{12}$$

$$\partial_x \psi^{(l)} - \partial_x \psi^{(l+1)} = 0. \quad (13)$$

Finally, due to the effect of surface tension, the normal stresses are balanced through it, where:

$$\boldsymbol{n}_l \cdot \| -p\mathrm{I} + \boldsymbol{\tau}_E^{(r)} \|_l^{(l+1)} \cdot \boldsymbol{n}_l = -\gamma_{l(l+1)} \nabla \cdot \boldsymbol{n}_l, \quad (14)$$

Here, the quantity $\gamma_{l(l+1)}$ indicates the surface tension of the fluid interfaces surface tension, and $\tau_E^{(r)}$ is the Maxwell stress tensor as a result of electrostatic forces

$$\boldsymbol{\tau}_E^{(r)} = \varepsilon^{(r)}(\boldsymbol{E}^{(r)}\boldsymbol{E}^{(r)} - \frac{1}{2}(\boldsymbol{E}^{(r)} \cdot \boldsymbol{E}^{(r)})I), \quad (15)$$

where, the symbol I denotes the identity tensor. The dynamic condition (14) is important for obtaining the characteristic stability equation later, therefore we will write this condition in terms of $\phi^{(r)}$ and $\psi^{(r)}$. To do this, we obtain the pressure by interpolating Equation (4) by (2) to be:

$$p^{(r)} = \eta_0^{(r)}\phi^{(r)} + \rho^{(r)}(\partial_t \phi^{(r)} + U_0^{(r)}\cos\Omega t \partial_x \phi^{(r)} - gy), \quad (16)$$

Therefore, the balance at the separating surfaces can be outlined in the form:

$$k^2\gamma_{l,l+1}h_l + \rho^{(l)}\partial_t\phi^{(l)} - \rho^{(l+1)}\partial_t\phi^{(l+1)} + \cos\Omega t\{\rho^{(l)}U_0^{(l)}\partial_x\phi^{(l)} - \rho^{(l+1)}U_0^{(l+1)}\partial_x\phi^{(l+1)}\} - \{\varepsilon^{(l)}E_0^{(l)}\partial_y\psi^{(l)} - \varepsilon^{(l+1)}E_0^{(l+1)}\partial_y\psi^{(l+1)}\} + \eta_0^{(l)}\phi^{(l)} - \eta_0^{(l+1)}\phi^{(l+1)} - g(\rho^{(l)} - \rho^{(l+1)})h_l = 0. \quad (17)$$

3 Lines of solutions

At this stage, we would like to study the stability of the hypothesized model since the dividing surfaces undergo a slight perturbation around their equilibrium position. The normal mode approach is employed to analyze linear stability performance (see Chandrasekhar [13]), where the occurrence of the disruption of the dividing surfaces can be indicated as:

$$y = (-1)^{(l+1)}H + \xi^{(l)}(t)\exp(ikx) + c.c. \quad (18)$$

Here, we assume that the influence of small wave disturbances on the allocating surfaces propagates in the positive x-direction, where only the linear limits are preserved and the higher degrees are neglected based on the linear stability theory [24, 26]. In the above equation, $\xi^{(l)}$ represents an arbitrary time-dependent quantity that controls the performance of the amplitude of the instabilities on the inner surfaces. Furthermore, k identifies the real wave number and the letter i denotes $\sqrt{-1}$, while c.c. denotes complex conjugate.

In the same vein, as discussed for interface deflection in Eq. (18), the stream and field functions in a fluid bulk can be expressed as follows:

$$(\phi^{(r)}, \psi^{(r)}) = \left(\hat{\phi}^{(r)}(y,t), \hat{\psi}^{(r)}(y,t)\right)\exp(ikx) + c.c. \quad (19)$$

Inserting Eq. (19) into Laplace's Eqs. (5), (8); the following solutions can be obtained:

$$\begin{pmatrix}\varphi^{(r)} \\ \chi^{(r)}\end{pmatrix} = \begin{pmatrix}A_1^{(r)}(t)\exp(-(-1)^j ky) + A_2^{(r)}(t)\exp((-1)^j ky) \\ B_1^{(r)}(t)\exp(-(-1)^j ky) + B_2^{(r)}(t)\exp((-1)^j ky)\end{pmatrix}\exp(ikx) + c.c. \quad (20)$$

Noting that the upper and lower plates are at rest, it means that the constants $A_1^{(1)}$, $A_1^{(3)}$, $B_1^{(1)}$and $B_1^{(3)}$ must be equal to zero, and in terms of $\xi^{(l)}$, the other measures are determined in view of the previous conditions at the interfaces.

4. Characteristic equations

The goal of this section is to investigate the influence of general surface distortions on the onset of a periodic speed applied to the liquid layers. As mentioned earlier, the normal stress tensor (17) is employed to obtain the characteristic equations, which are the relations that describe the behavior of the interfaces. By interpolating Eqs. (20) in the previous dynamic condition, we obtained in terms of the amplitude $\xi^{(l)}$, two coupled Mathieu relations. These equations have damping terms and complex coefficients and can be expressed as:

$$F_l(\xi''^{(1)}(t), \xi'^{(1)}(t), \xi^{(1)}(t), \xi''^{(2)}(t), \xi'^{(2)}(t), \xi^{(2)}(t)) = 0. \quad (21)$$

Based on these relationships, the stability of the interface and thus the stability of the system as a whole is controlled.

Uniform Stream: Dealing with these equations, we will first discuss the case of uniform velocity. This is in the absence of periodicity of speed, and for this reason, Ω degenerates to zero in the above analysis. Accordingly, Mathieu equations turn into linear differential equations with constant coefficients. Therefore, we can impose the solution in the form of a growth rate as follows:

$$\xi^{(l)} = \mathrm{A}^{(l)}\exp(i\Theta t), \quad (22)$$

where $\mathrm{A}^{(l)}$ indicates the constant of integration. With the aid of this solution and in the light of the previous Mathieu equations, we can reach a dispersion equation that designates the perturbed motion, which is:

$$\Theta^4 + (\varsigma_{11} + i\varsigma_{12})\Theta^3 + (\varsigma_{21} + i\varsigma_{22})\Theta^2 + (\varsigma_{31} + i\varsigma_{32})\Theta + \varsigma_{41} + i\varsigma_{42} = 0, \quad (23)$$

where the measurements ς's are obvious from the context. In terms of Θ and k, we find that Eq. (23) is labeled as a dispersion equation with complex coefficients describing linear motion of uniform velocity. It is important to discuss here that the system represented by this equation is stable only if all the roots of this equation are real, or that there are at least two conjugate complex roots and thus we obtain unstable motion.

In the following, we will carry out a numerical study to clarify the concept of stability for some physical variables under study. For this purpose and to better understand the stability performance, all physical quantities have been placed in a non-dimensional form based on the following hypotheses. The dielectric constant and the density ratios are created dimensionless through $\hat{\varepsilon}^{(1)} = \varepsilon^{(1)}/\varepsilon^{(2)}$, $\hat{\varepsilon}^{(2)} = \varepsilon^{(3)}/\varepsilon^{(2)}$ and $\hat{\rho}^{(1)} = \rho^{(1)}/\rho^{(2)}$, $\hat{\rho}^{(2)} = \rho^{(3)}/\rho^{(2)}$, while the speed and its potential function are created by $\sqrt{Hg}$ and $H\sqrt{Hg}$. Furthermore, the field and the electric potential are ended dimensionless by $\sqrt{Hg\rho^{(2)}/\varepsilon^{(2)}}$ and $H\sqrt{Hg\rho^{(2)}/\varepsilon^{(2)}}$, and the permeability of the media by H^2Q. Finally, the Weber number is defined as $W_l = \gamma_l/H^2 g\rho^{(2)}$, ($l = 1,2$).

Fig. 2 displays the effect of the applied electric field on the stability performance of the fluid layers. All other physical quantities are kept constant as indicated in the caption of this graph. As earlier discussed, the four roots of the characteristic Equation 23 versus the wave number were established in the parts of this figure, which represent the case of uniform velocities.

The field's value of 0.1 was selected in Fig. 2(a). It was shown that in the range $0 < k < 0.3$, all the roots of the dispersion equation are real, indicating that we are working with a steady motion. On the other hand, one complex root in the interval $0.3 < k < 3.5$ indicates unstable waves. We found that the stable zone, which is characterized by the appearance of all four roots, grew to include the distance $k < 0.33$ by expanding the value of the field to 0.4 in the second part of Fig. 2. This indicates that the stability of the wave motion is stimulated by the electric field. The field was increased once more in the third and last section of this graph to validate its stabilizing effect. As a result of this expansion, the unstable region contracted and the stable distance increased to reach $k \approx 0.35$, indicating that we are dealing with stable waves. This implies that a portion of the kinetic energy wave motion has shifted to the field, improving stability, and this is a plausible physical explanation [1, 27].

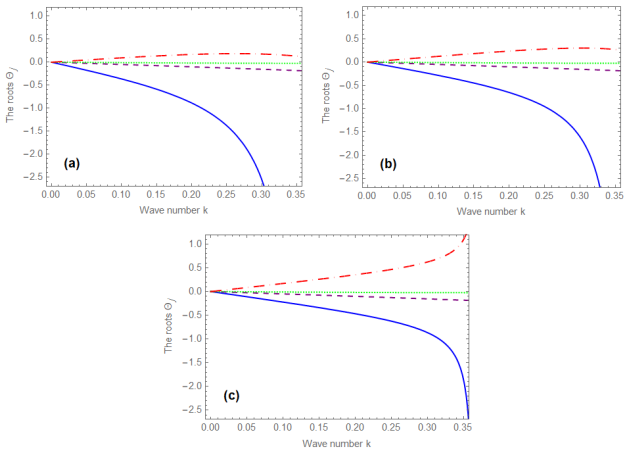

Fig. 2. Plot of roots of (23) against the wave number k, related to a system with $L_1 = 0.5$, $L_2 = 0.8$, $U_0^{(1)} = 0.5$, $U_0^{(2)} = 0.3$, $U_0^{(3)} = 0.6$, $\hat{\varepsilon}^{(1)} = 0.6$, $\hat{\varepsilon}^{(2)} = 0.5$, $\hat{\rho}^{(1)} = 0.6$, $\hat{\rho}^{(2)} = 0.7$ $Q^{(1)} = 0.5$, $Q^{(2)} = 0.8$, $Q^{(3)} = 0.4$, with $E_0^{(1)} = 0.1$, 0.4 and 0.7 of the partitions (a), (b) and (c), respectively.

Fig. 3 was created in a three-dimensional system from the perspective of the height of the surface wave, where the horizontal direction of the waves' movement and the elevation of the upper interface were plotted against time. The parts of this figure represent three different values of the upper porous permeability for comparison while preserving the values of other variables as mentioned in the previous figure. A general inspection of this figure demonstrates that increasing the upper permeability $Q^{(1)}$ to a value of 0.4 in Fig. 2(b) leads to a contraction of the crests and troughs of the waves. However, another increase in $Q^{(1)}$ to become 0.7 in the third part of this graph leads the waves to return in expanding of troughs and crests. Zakaria et al [9] in their study of the instability of a viscous liquid sheet under the influence of a tangential electric field.

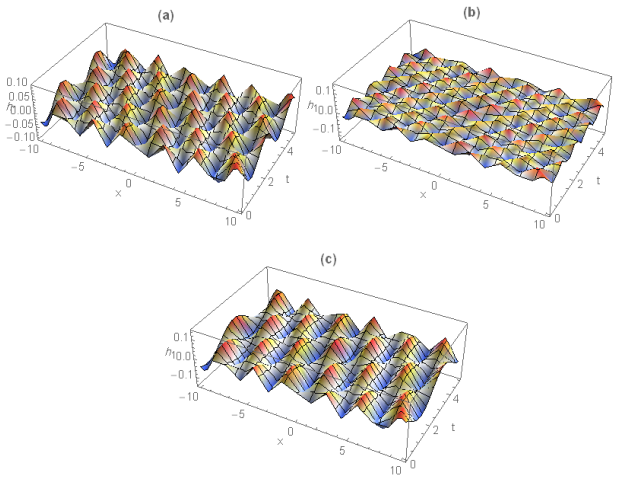

Fig. 3. Upper interface elevation at $y = 1$, such that the upper permeability $Q^{(1)} = 0.1 = 0.4$, and 0.7 are indicated for (a), (b), and (c), respectively.

Periodic Velocity: Returning to the general case when the oscillatory speed is operating. In this regard, the study of stability criterion changes radically, and dispersion Equation (21) is again the focus of the study. It isn't easy to obtain an exact solution to such equations; therefore, we need to deal with one of the approximate methods. One of these successful approaches is the method of multiple time scales [26].

In the procedures of this method, the time scale is expressed in the independent quantities $t_n = \epsilon t$,$n = 0,1,2$, where the small amount ϵ describes the steepness ratio of the wave. Here, t_0 is discussed as the slower variable, which is appropriate for the faster ones t_1, and t_2. In the light of this hypothesis, the differentials with respect to time are formulated in the form of the following expansions:

$$\partial_t \equiv \partial_{t_0} + \epsilon\partial_{t_1} + \ldots \quad \text{and} \quad \partial_{t^2}^2 \equiv \partial_{t_0^2}^2 + 2\epsilon\partial_{t_0 t_1}^2 + \ldots, \qquad (24)$$

Reliant on the smallness of the arbitrary dimensionless quantity ϵ, the amplitude of the periodic forces can be designated as $U_0^{(r)} = \epsilon\tilde{U}_0^{(r)}$. The investigation then obeys the standard perturbation technique and refrains from using secular terms, which is now more appropriate for expressing the outcome in a complex formula.

It is now preferable to express $\xi^{(l)}$ as an expansion in the following feature:

$$\xi^{(l)}(t,\epsilon) = \xi_0^{(l)}(t_0,t_1) + \epsilon\xi_1^{(l)}(t_0,t_1) + \ldots, l = 1,2. \qquad (25)$$

By inserting the expansions (24) and (25) into Equations (21) and knowing that $\xi^{(l)}$ is independent of ϵ, we can compare the coefficients of the similar powers of ϵ. In this case, we obtain inhomogeneous equations, which are solved successively based on the solution of the previous order. Eliminating the secular terms from specified uniform solutions generates what is known as the solvability conditions, which correspond to the terms containing the expression $\exp(i\Theta t_0)$.

These solvability requirements are divided into two categories: non-resonance, which occurs when the frequency Ω is far from the frequency Θ, and resonance, which occurs when Ω is approaching Θ. The non-resonant case is subjected to the following solvability condition:

$$(f_1^{(1)} + if_2^{(1)})\partial_{t_1}A_1 + (s_1^{(1)} + is_2^{(1)})A_1 = 0. \qquad (26)$$

This specification shows that the sheet is stable if:

$$f_1^{(1)}s_1^{(1)} + f_2^{(1)}s_2^{(1)} \geq 0 \tag{27}$$

In the case of resonance, the closeness between Ω and Θ can be expressed by defining a detuning factor $\lambda^{(1)}$, where:

$$\Omega = 2\varpi + 2\epsilon\lambda^{(1)}, \tag{28}$$

and so the solvability conditions reads

$$(f_1^{(1)} + if_2^{(1)})\partial_{t_1}A_l + (s_1^{(1)} + is_2^{(1)})A_l + (h_1^{(1)} + ih_2^{(1)})\bar{A}_1\exp(2i\lambda^{(1)}t_1) = 0. \tag{29}$$

Herein, $\bar{A}_1$ is the complex conjugate of A_1. The solution of the above equation as can be resolved as:

$$A_1 = (m_1^{(1)} + im_2^{(1)})\exp[(\tilde{\Theta} + i\lambda^{(1)})t_1] \tag{30}$$

Inserting Eq. (30) into (29), and keeping in mind that $\tilde{\Theta}$ and $\lambda^{(1)}$ are real, the real and imaginary terms can be expressed as $m_1^{(1)}$ and $m_2^{(1)}$ which are proportional to $\exp(\tilde{\Theta}t_1)$. At this stage, a dispersion equation is produced where the coefficient matrix must be zero for non-trivial solutions. This relation has the form:

$$\tilde{\Theta}^2 + 2f^{(1)^{-1}}(f_1^{(1)}s_1^{(1)} + f_2^{(1)}s_2^{(1)})\tilde{\Theta} + \lambda^{(1)^2} + 2f^{(1)^{-1}}(f_1^{(1)}s_1^{(1)} - f_2^{(1)}s_2^{(1)})\lambda^{(1)} + f^{(1)^{-1}}(s_1^{(1)^2} + s_2^{(1)^2} - h_1^{(1)^2} - h_2^{(1)^2}) = 0, \tag{31}$$

where, $f^{(1)} = (f_1^{(1)^2} + f_2^{(1)^2})$. Eq. (31) is the desired dispersion relation according to which the stability in the resonance state is investigated. It is important to note that the sign of $\tilde{\Theta}$ directly influences the wave's growth or decay [24, 26]. Therefore, the stability of the system associated with Eq. (31) is achieved under two conditions. The first is the same as the previous condition in the case of non-resonance, and the second can be formulated in the form:

$$\lambda^{(1)^2} + 2f^{(1)}(f_1^{(1)}s_2^{(1)} - f_2^{(1)}s_1^{(1)})\lambda^{(1)} + f^{(1)}(s_1^{(1)^2} + s_2^{(1)^2} - h_1^{(1)^2} - h_2^{(1)^2}) \geq 0 \tag{32}$$

The two roots for solving the quadratic Eq. (32) signify transition curves that can be drawn with the wave number, for example, to formulate ($\lambda^{(1)} - k$) plane. These branches appear as ϵ approaches zero in Eq. (28) and divide the plane into stable and unstable regions. Matching Fleque's theory [26], the space confined between these two roots has an unstable feature;on the contrary, the spaces outside it express the stability of the system.

To discuss the effect of some physical variables in the current problem, a numerical representation of the previous resonance cases is formulated. Eq. (32) controls the stability performance of the fluid system, which requires numerical simulation of the same inputs handled in the case of uniform velocity referred to in the previous item. Numerical applications of the transition borders $\lambda_{1,2}^{(1)}$, given by the roots of Eq. (32) in the case of $\Omega \approx \Theta$, are constructed in Figs. 4-6. The instability is due to the equilibrium between the quantity Ω and the parameter Θ. In these figures, numerical research was organized to determine the stable regions and their unstable counterparts. The stable areas are subject to the validity of inequalities (27) and (32). The spaces that express the stability of waves are denoted by the letter S, while the unstable zones are marked by the symbol U.

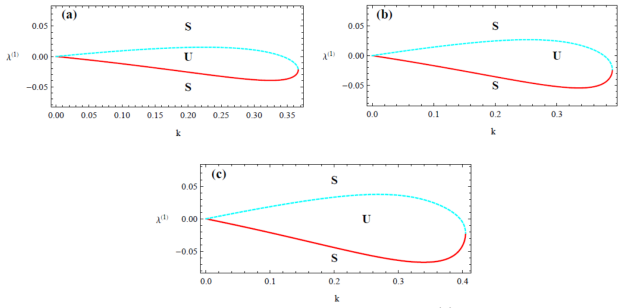

Fig. 4. The system in Fig. 2 is repeated, but for $U_0^{(1)}$= 2, 5, and 8 of the pictures (a), (b), and (c), respectively.

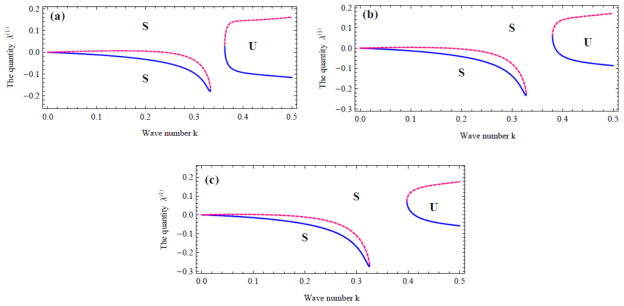

Fig. 5. Plot in the ($\lambda^{(1)} - k$) plane, in view of the root of Eq. (32), at $\hat{\varepsilon}^{(3)}$= 0.6, 1.4 and 1.8 of the parts (a), (b) and (c), respectively.

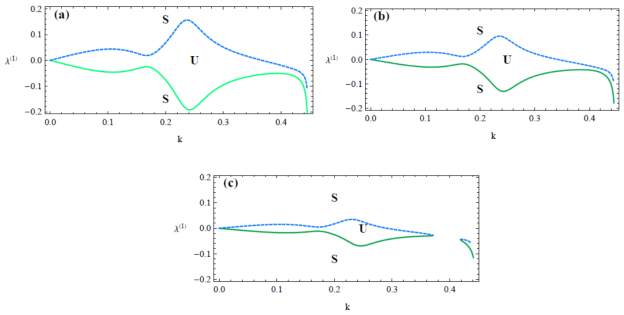

Fig. 6. Stability picture $\lambda^{(1)}$ as a function of k, for the identical system specified in Fig. 2, with $E_0^{(1)}$= 0.3, 0.5 and 0.7 of the panels (a), (b) and (c), respectively.

To investigate the effect of velocity on the stability of the fluid sheet, the three parts of Fig. 4 were constructed at three different values of speed in the upper layer for comparison. These values 2, 5, and 8 correspond to Figs. 4(a), 4(b), and 4(c), respectively and the remaining values are left as they appear in Fig. 2. As previously mentioned, the images of these graphs, which are represented by the $\lambda_{1,2}^{(1)} - \mathrm{k}$ plane, are the area confined between characteristic curves $\lambda_{1,2}^{(1)}$ which are areas subject to an unstable system. On the other hand, all the points outside these curves encounter waves that have a stable nature.

Now, by progressing from Fig. 4(a) to (b), and comparing the stable regions with their unstable counterparts, it is evident that the increase in the speed of the upper film led to the reduction of the stable regions at the expense of the unstable spaces. From here, it can be concluded that increasing the speed, interferes with the stability of the system. Moreover, as the velocity continues to increase in part(c), we discovered that the unstable role of this velocity continues. Therefore, it can be concluded that the speed of the

upper layer works to destabilize the waves and thus the fluid sheet becomes completely unstable.

Below, we want to elucidate how the fluid sheet stability is affected by the ratio of the dielectric constants between the middle film and the upper layer.

Fig. 5, which shows the transition curves as a function of the wave number, was made for this purpose. As was mentioned in the case of Fig. 2, all physical quantities were held to schedule, and the dielectric constant was converted into three appropriate values corresponding to the three images in this figure, which are in the order of 0.6, 1.4, and 1.8. In the images of this figure, it can be seen that each part contains two unstable regions that correspond to the rest of the stable space, and by matching the three sections of the figure, we discovered that the stable voids increase due to an increase in the dielectric constant.On the other hand, a noticeable shrinkage appears in the unstable regions, which proves that the dielectric constant gives brightness to the stability of the waves.

In Portions(a), (b), and (c) of Fig. 6, we seek the impact of the electric field on the movement of waves inside the fluid sheet. Numerical applications similar to those in Fig. 2 have been carried out. The values 0.3, 0.5, and 0.5 of the electric field were chosen to illustrate the extent of the change in the construction of these parts. Based on an analysis of the unstable regions and areas expressing system stability, the following conclusion can be drawn, which is consistent with earlier discussions: the electric field plays a significant and useful function in stabilizing the fluid layers. One explanation for the field performance may be physically interpreted as some kinetic energy has been absorbed into the liquid sheet, thereby assisting in the stabilization of fluid layers. Similar significances for the electric field impact were drawn in [7, 9].

5. Concluding remarks

The aim of this work is to investigate the linear stability of a fluid sheet moving in porous media. The sheet consists of three non-viscous, non-miscible fluids with different physical properties. These fluids are bounded from above and below by two fixed plates and contain two interfaces. The liquid sheet is exposed to a horizontal electric field in the presence of a periodic velocity in the direction of fluid movement.

Depending on the theory of linear stability, the system of equations governing the system and the associated boundary and interface conditions lead to two Mathieu type equations. These coupled equations have damping complex coefficients and employed to restrain the stability of the system. Since it is challenging to find exact solutions for these kinds of equations, we are searching for a method to find approximate solutions. Approximate solutions were achieved by means of method of multiple scales, where the stability presentation in resonance situations or not was examined. An essential characteristic of this approach is that transition curves are accomplished analytically. The characteristic curves separating stable zones from all unstable points are recognized.

In locating all the physical quantities utilized in a non-dimensional form, a numerical examination was conducted to investigate the stability of the imposed system. In the absence of periodicity of speed under the influence of the regular electric field, and having obtained the numerical survey, it was noted that the electric field enhances the stability of the fluid sheet, while a dual performance is established for the porosity of the top film. As the periodicity of the stream is switched on, the stable and unstable regions delineated by the characteristic curves are traced. It was observed that the speed of the top layer works to destabilize the waves, while the dielectric constant gives a boost to the stability of the waves. It is also shown that the electric field plays an important and useful role in maintaining the fluid layer stability.

Finally, in future analyses, our research can be enlarged to discuss motion through porous substrates as well as wavy and slippery planes. Also, viscoelastic liquids are useful materials to investigate the impact of both relaxation and retardation times as well as electric or magnetic fields with surface charge.

Acknowledgments

This work was supported and funded by "The Research Program of Public Authority for Applied Education and Training in Kuwait", Project No. (TS-23-05).

References

[1] O. Ozen, N. Aubry, D. T. Papageorgiou, and P. G. Petropoulos, "Electrohydrodynamic linear stability of two immiscible fluids in channel flow," *Electrochim. Act.*, vol. 51, no. 25, pp. 5316–5323, Jul. 2006, doi: 10.1016/j.electacta.2006.02.002.

[2] F. Li, O. Ozen and N. Aubry, "Linear stability of a two-fluid interface for electrohydrodynamic mixing in a channel", *J. Fluid Mech.* vol. 583, pp. 347-377, Jul. 2007.

[3] K. C. Sahu and O. K. Matar, "Stability of plane channel flow with viscous heating", *ASME J Fluids Eng.,* vol. 132, no. 1, Art. no. 011202, Jan. 2010.

[4] D. A. DiCarlo, "Stability of gravity-driven multiphase flow in porous media: 40 Years of advancements," *Water Resourc. Res.*, vol. 49, no. 8, pp. 4531–4544, Aug. 2013, doi: 10.1002/wrcr.20359.

[5] K. Zakaria and S. A. Alkharashi, "Linear stability of a thin film flow along permeable wall under alternating electric field," *Z Angew Math Mech*, vol. 96, no. 10, pp. 1184–1204, Oct. 2016, doi: 10.1002/zamm.201400209.

[6] S. A. Alkharashi and Y. Gamiel, "Stability characteristics of periodic streaming fluids in porous media," *Theor Math Phys*, vol. 191, no. 1, pp. 580–601, Apr. 2017, doi: 10.1134/S0040577917040092.

[7] S. A. Alkharashi, "A model of two viscoelastic liquid films traveling down in an inclined electrified channel," *Appl. Mathem. Computat.*, vol. 355, pp. 553–575, Aug. 2019, doi: 10.1016/j.amc.2019.03.005.

[8] K. Gautam, P. A. L. Narayana, and Kirti Chandra Sahu, "Linear instability driven by an electric field in two-layer channel flow of Newtonian and Herschel–Bulkley fluids", *J. Non-Newton. Fluid Mechan.*, vol. 285, 104400, Nov. 2020.

[9] K. Zakaria, H. Kamel and Y. Gamiel, "Instability of a viscous liquid sheet under the influence of a tangential electric field", *Alexandria Eng. J.*, vol. 61, no. 7, pp. 5169-5181, Jul. 2022.

[10] L.-J. Yang, B.-R. Xu, and Q.-F Fu, "Linear instability analysis of planar non-Newtonian liquid sheets in two gas streams of unequal velocities", *J. Non-Newton. Fluid Mech.,* Vol. 167–168, pp. 50–58, Jan. 2012.

[11] K. S. Fayazov and I. O. Khajiev, "Estimation of conditional stability of the boundary-value problem for the system of parabolic equations

with changing direction of time", *Rep. Mathem. Phys.,* vol. 88, no. 3, pp. 419-431, Dec. 2022.

[12] S. A. Alkharashi, Kh. Al-Hamad and A. Alrashidi, "An approach based on the porous media model for multilayered flow in the presence of interfacial surfactants", *Pramana – J. Phys.,* vol. 96, no. 2, Art. no. 140, Sep. 2022.

[13] S. Chandrasekhar, *Hydrodynamic and hydromagnetic stability*, Dover ed. New York: Dover Publications, 1981.

[14] M. Iervolino, J.-P. Pascal, and A. Vacca, "Instabilities of a power–law film over an inclined permeable plane: A two–sided model," *J. Non-Newton. Fluid Mechan.*, vol. 259, pp. 111–124, Sep. 2018, doi: 10.1016/j.jnnfm.2018.03.011.

[15] M. A. Sirwah and K. Zakaria, "Dynamics of surface waves of a ferrofluid film", *Wave Mot.*, vol. 84, pp. 8-31, Jan. 2019.

[16] S. A. Roberts and S. Kumar, "AC electrohydrodynamic instabilities in thin liquid films", *J. Fluid Mech*., vol. 63, pp. 255-279, Jul. 2009.

[17] S. A. Alkharashi, *The effect of the porosity property on the dynamics of some fluids*, Master thesis, Tanta University, 2007.

[18] Y. Liu, M. Dong, and X. Wu, "Receptivity of inviscid modes in supersonic boundary layers to wall perturbations," *J Eng Math*, vol. 128, no. 1, Art. no. 20, Jun. 2021, doi: 10.1007/s10665-021-10124-4.

[19] L. Kahouadji *et al.*, "A numerical investigation of three-dimensional falling liquid films," *Environ Fluid Mech*, vol. 22, no. 2–3, pp. 367–382, Jun. 2022, doi: 10.1007/s10652-022-09849-2.

[20] K. Zakaria, M. A. Sirwah, K. M. Elmorabie, and S. N. Eldeen, "Sloshing waves in electrified fluid layers in an excited rectangular container," *Appl. Ocean Res.*, vol. 91, Art. no 101902, Oct. 2019, doi: 10.1016/j.apor.2019.101902.

[21] S. A. Alkharashi, *Stability of viscous fluids in the presence of the porosity effect*, Ph.D. thesis Tanta University, 2012.

[22] G. Ravi Kiran, V. Radhkrishna Murthy, and G. Radhakrishnamacharya, "Pulsatile flow of a dusty fluid thorough a constricted channel in the presence of magnetic field," *Mater. Today: Proceed.*, vol. 19, pp. 2645–2649, Jun. 2019, doi: 10.1016/j.matpr.2019.10.116.

[23] H. A. Hosham and N. M. Hafez, "Global Dynamics and Bifurcation Analysis for the Peristaltic Transport Through Nonuniform Channels," *J. Computat. Nonlinear Dynam.*, vol. 17, no. 6, Art. no. 061001, Jun. 2022, doi: 10.1115/1.4053668.

[24] P. G. Drazin and W. H. Reid, *Hydrodynamic Stability*, 2nd ed. Cambridge University Press, 2004. doi: 10.1017/CBO9780511616938.

[25] S. A. Alkharashi and M. A. Sirwah, "Dynamical responses of inclined heated channel of MHD dusty fluids through porous media," *J. Eng. Math.*, vol. 130, no. 1, p. 5, Oct. 2021, doi: 10.1007/s10665-021-10160-0.

[26] A. H. Nayfeh and D. T. Mook, *Nonlinear Oscillations*, 1st ed. Wiley, 1995. doi: 10.1002/9783527617586.

[27] K. Zakaria, M. A Sirwah, and S. Alkharashi, "Temporal stability of superposed magnetic fluids in porous media," *Phys. Scr.*, vol. 77, no. 2, Art. no. 025401, Feb. 2008, doi: 10.1088/0031-8949/77/02/025401.

[28] A. Assaf and S. A. Alkharashi, "Hydromagnetic instability of a thin viscoelastic layer on a moving column," *Phys. Scr.*, vol. 94, no. 4, Art. no. 045201, Apr. 2019, doi: 10.1088/1402-4896/aaf948.

[29] M. A. Sirwah and K. Zakaria, "Nonlinear evolution of the travelling waves at the surface of a thin viscoelastic falling film," *Appl. Mathemat. Modell.*, vol. 37, no. 4, pp. 1723–1752, Feb. 2013, doi: 10.1016/j.apm.2012.04.006.

[30] S. A. Alkharashi, A. Assaf, Kh. Al-Hamad and A. Alrashidi, "Performance Evaluation of Insoluble Surfactants on the Behavior of Two Electric Layers", *J. Appl. Fluid Mechan.,* vol. 12 no. 2, pp. 573–586, Mar. 2019, doi: 10.29252/jafm.12.02.28618.

[31] N. M. Hafez and A. Assaf, "Electrohydrodynamic stability and heat and mass transfer of a dielectric fluid flowing over an inclined plane through porous medium with external shear stress," *Eur. Phys. J. Plus*, vol. 138, no. 1, p. 28, Jan. 2023, doi: 10.1140/epjp/s13360-022-03615-5.

[32] S. A. Alkharashi and W. Alotaibi, "Structural stability of a porous channel of electrical flow affected by periodic velocities," *J Eng Math*, vol. 141, no. 1, Art. no 3, Aug. 2023, doi: 10.1007/s10665-023-10278-3.